

Tracing of particulate organic C sources across the terrestrial-aquatic continuum, a case study at the catchment scale (Carminowe Creek, South West England)

M. Glendell^{1*}, R. Jones², J.A.J. Dungait³, K. Meusburger⁴, A.C. Schwendel⁵, R. Barclay², S. Barker⁶, S. Haley², T.A. Quine², J. Meersmans⁷

1. The James Hutton Institute, Craigiebuckler, Aberdeen AB15 8QH, UK
2. University of Exeter, Geography - College of Life and Environmental Sciences, Exeter EX4 4RJ, UK
3. Sustainable Agriculture Science, Rothamsted Research, North Wyke, Okehampton, Devon, EX20 2SB, UK
4. Environmental Geosciences, University of Basel, Bernoullistrasse 30, 4056 Basel, Switzerland
5. School of Humanities, Religion & Philosophy, York St John University, Lord Mayor's Walk, York, YO31 7EX, UK
6. Environment and Sustainability Institute, University of Exeter, Penryn Campus, Penryn, Cornwall TR10 9FE
7. School of Water, Energy and Environment, Cranfield University, Bedford, MK43 0AL, UK

* Corresponding author:

The James Hutton Institute, Craigiebuckler, Aberdeen AB15 8QH, Scotland, UK,
Miriam.Glendell@hutton.ac.uk, tel: +44(0)1224 395 320, fax: +44 (0)844 928 5429

Abstract

Soils deliver crucial ecosystem services, such as climate regulation through carbon (C) storage and food security, both of which are threatened by climate and land use change. While soils are important stores of terrestrial C, anthropogenic impact on the lateral fluxes of C from land to water remains poorly quantified and not well represented in Earth system models. In this study, we tested a novel framework for tracing and quantifying lateral C fluxes from the terrestrial to the aquatic environment at a catchment scale. The combined use of conservative plant-derived geochemical biomarkers *n*-alkanes and bulk stable $\delta^{13}\text{C}$ and $\delta^{15}\text{N}$ isotopes of soils and sediments allowed us to distinguish between particulate organic C sources from different land uses (i.e. arable and temporary grassland *vs.* permanent grassland *vs.* riparian woodland *vs.* river bed sediments) ($p < 0.001$), showing an enhanced ability to distinguish between land use sources as compared to using just *n*-alkanes alone. The terrestrial-aquatic proxy (TAR) ratio derived from *n*-alkane signatures indicated an increased input of terrestrial-derived organic matter (OM) to lake sediments over the past 60 years, with an increasing contribution of woody vegetation shown by the $\text{C}_{27}/\text{C}_{31}$ ratio. This may be related to agricultural intensification, leading to enhanced soil erosion, but also an increase in riparian woodland that may disconnect OM inputs from arable land uses in the upper parts of the study catchment. Spatial variability of geochemical proxies showed a close coupling between OM provenance and riparian land use, supporting the new conceptualization of river corridors (active river channel and riparian zone) as critical zones linking the terrestrial and aquatic C fluxes. Further testing of this novel tracing technique shows promise in terms of quantification of lateral C fluxes as well as targeting of effective land management measures to reduce soil erosion and promote OM conservation in river catchments.

Keywords: lateral carbon fluxes, sediment fingerprinting, biomarkers, *n*-alkanes, bulk stable ^{13}C and ^{15}N isotopes

1. Introduction

Soils are critical to human wellbeing and deliver crucial ecosystem services, including climate regulation and food security (Adhikari and Hartemink, 2016; Mouchet et al., 2016). However, since the onset of agriculture, human activities have greatly altered soil processes at a global scale, with consequences for the essential functions of soils to sequester and store carbon (C), recycle nutrients and resist soil erosion (Amundson et al., 2015). As soils represent the largest terrestrial store of organic C, more than three times as much as either the atmosphere or terrestrial vegetation (Schmidt et al., 2011), these anthropogenic interventions have also impacted the scale of the lateral fluxes of C from land to inland waters (Lauerwald et al., 2015; Tian, 2015; Wohl et al., 2017).

However, the fluxes of C from land to ocean remain poorly quantified and not fully accounted for in the current generation of Earth system models (Regnier et al., 2013). While over the past decade, the understanding of rivers has been revised from ‘inert pipes’ simply transporting C from land to the ocean to ‘active agents’ (Battin et al., 2009; Cole et al., 2007; Wohl et al., 2017), which play an important role in receiving, transporting and processing an estimated 2.7-2.9 Pg C yr⁻¹ C in their watersheds (Regnier et al., 2013), ‘similar in magnitude to the net ecosystem C balance of the terrestrial ecosystems’ (Aufdenkampe et al., 2011 p. 53), the magnitude, spatiotemporal patterns and controls on C fluxes from land to ocean remain poorly quantified (Regnier et al., 2013; Wohl et al., 2017). While there is a growing understanding of the magnitude of global C exports from rivers to the ocean (Li et al., 2017; Ludwig et al., 2011; Tian et al., 2015), estimates of CO₂ evasion from inland waters (Lauerwald et al., 2015; Raymond et al., 2013) and sediment burial in aquatic ecosystems (Maavara et al., 2017; Tranvik et al., 2009) are still uncertain. However, the largest uncertainties are associated with the scale of the total lateral C fluxes from land to inland waters, with recent research suggesting that previous estimates may have largely over-estimated C accumulation in terrestrial ecosystems (the terrestrial C sink) due to under-estimation of this lateral C export (Nakayama, 2017). Therefore, there is a need to better understand the scale of the anthropogenic impact on these lateral C fluxes from land to water (Regnier et al., 2013; Wohl et al., 2017), as well as the processes involved in the loss and preservation of C along the terrestrial-aquatic continuum (Marín-Spiotta et al., 2014), to properly represent these processes and predict the present and future contribution of aquatic C fluxes to the global C budget (Aufdenkampe et al., 2011; Battin et al., 2009; Cole et al., 2007; Regnier et al., 2013).

Over the past decades, the awareness of the importance of soils in the functioning of many vital ecosystem services, including climate change mitigation, food security, water resource management and flood protection has greatly increased (Schroter et al., 2005). Nevertheless, in many parts of the world where soil erosion rates exceed soil production, the sustainable provision of these ecosystem services is under pressure (Alewell, et al., 2015; Amundson et al., 2015; Panagos et al., 2015; Verheijen et al., 2009). The intensification of agriculture, particularly over the past 60 years, has led to an exponential increase in sediment and organic matter (OM) fluxes within agricultural catchments (Glendell and Brazier, 2014; Graeber et al., 2015), with important consequences for on-site impacts, such as soil productivity, and off-site impacts, in terms of nutrient pollution and sedimentation of water bodies (Tilman et al., 2002).

Hence, conservation of soil organic matter (SOM; which contains ~60% SOC) remains critical for sustaining soil productivity and food security in a changing world (e.g. Amundson et al., 2015; Meersmans et al., 2016) and for mitigating the acknowledged wide-scale impacts of enhanced sedimentation and associated nutrient pollution on the ecological status of water bodies and drinking water quantity and quality (Bilotta and Brazier, 2008; Glendell et al., 2014a; Rickson, 2014; Schoumans et al., 2014).

Tracing and quantifying the sources of sediment and particulate organic C in the fluvial environment is, therefore, key to supporting sustainable land management decisions and maintaining ecosystem services. To date, most tracing techniques to apportion sediment sources in fluvial environments applied in river management studies have used physical sediment characteristics, geochemical properties, fallout radionuclides or mineral magnetic properties. However, these tracers are not able to distinguish sources between specific land uses, which are essential to inform mitigation measures and catchment management (Guzman et al., 2013; Owens et al., 2016; Smith et al., 2015; Walling, 2013). Conversely, examination of the provenance of sediment-bound OM using plant-specific biomarkers has been established in paleo-ecological and marine sciences for some time (e.g. Galy et al., 2011; Meyers and Lallier-Vergès, 1999; Meyers, 2003; Tolosa et al., 2013; Zech et al., 2012). While a number of studies to date have sought to apply one or more biomarkers to understand lateral C dynamics at the continental margins (e.g. Feng et al., 2015; Galy et al., 2011; Tao et al., 2016), few studies have applied this approach to inland waters, especially headwaters, which may cumulatively play an important role in lateral C export due to their spatial extent and close terrestrial – aquatic coupling. Therefore the application of biomarkers, especially aliphatic (saturated straight-chained) compounds such as *n*-alkanes (Chen et al., 2016, 2017; Cooper et al., 2015; Puttock et al., 2014) and *n*-carboxylic acids (fatty acids) (Alewell et al., 2016; Blake et al., 2012; Reiffarth et al., 2016), is now being examined as a new potential tool for attribution of sediment and C provenance in river catchments, with a potential to attribute organic matter sources to specific land uses, such as forest, arable and pasture.

N-alkanes are naturally occurring hydrocarbons which are relatively recalcitrant and more resistant to microbial decomposition than other functionalized plant-derived lipids, e.g. fatty acids or sterols (Ranjan et al., 2015). They are vegetation-specific neutral lipids derived from plant waxes with different numbers of C atoms in the aliphatic molecule that are indicative of different provenances of OM (Eglinton, 1962). In general, long-chain (C₂₇-C₃₁) *n*-alkanes are derived from epicuticular plant waxes of terrestrial plants (Galy et al., 2011; Puttock et al., 2014), medium chain-length (C₂₁-C₂₅) *n*-alkanes are produced by lower plants and aquatic macrophytes (Fang et al., 2014; Meyers, 2003; Tolosa et al., 2013), while short chain-length (C₁₅-C₁₉) *n*-alkanes are typically derived from aquatic algae (Meyers, 2003). Both individual *n*-alkanes as well as different chain-length ratios have been used in paleo-ecological studies to attribute OM sources over decadal to millennial timescales (Ranjan et al., 2015; Zech et al., 2013, 2012). As *n*-alkane signatures are altered by land use change, they are ideally suited to track changing OM sources from eroded soils and sediments over time (Chen et al., 2016).

With these naturally occurring biomarkers (and their compound-specific isotopic signatures where vegetation sources with contrasting $\delta^{13}\text{C}$ values are evident) emerging as the new

potential tools for tracing of SOM in catchment studies, a key challenge lies in establishing their effectiveness to act as land-management specific tracers of fluvial OM over decadal timescales (Alewell et al., 2016; Cooper et al., 2015). As these new techniques are still in their infancy (Owens et al., 2016) and require further development and testing, in this work we aim to investigate the suitability of *n*-alkane biomarkers within an inter-disciplinary context, beyond the traditional confines of soil science alone (Brevik et al., 2015; Owens et al., 2016; Smith et al., 2015).

Therefore, this pilot study aims to evaluate the combined use of *n*-alkanes, bulk stable $\delta^{13}\text{C}$ and $\delta^{15}\text{N}$ isotopes and their ratios (Collins, et al., 2014, 2013; Meyers and Lallier-Vergès, 1999; Meyers, 2003; Ranjan et al., 2015) to advance the current understanding of the temporal variability of lateral C fluxes from the terrestrial to the aquatic ecosystem in relation to changing land management practices, over the past century. Our aims were to i) test the ability of conservative *n*-alkane biomarkers and soil and sediment bulk stable $\delta^{13}\text{C}$ and $\delta^{15}\text{N}$ isotopes to distinguish between terrestrial and aquatic OM sources, ii) understand the impact of land use on the spatial variability of OM provenance in river bed sediments and iii) on OM accumulation in lake bed sediments, iv) test a methodology for quantifying the temporal variability and the magnitude of lateral C fluxes from land to water at catchment scales.

2. Material and Methods

2.1 Study site

The Carminowe Creek study catchment, located in southwest England (50°4' W 5°16'), covers c. 4.8 km² at an altitude range of 0-80 m above sea level (Fig. 1). The catchment outlet drains into a large freshwater lake Loe Pool (50 ha) that is separated from the Atlantic Ocean by a natural shingle barrier, thus creating a relatively closed natural hydrological system. The study catchment comprises two main streams (Northern and Southern subcatchments) with a joint outlet into the south-western branch of Loe Pool. The average total annual rainfall is approximately 1000 mm and mean annual temperature is approximately 11°C (<http://www.metoffice.gov.uk/public/weather/climate/>). Bedrock geology comprises silt-, sand- and mudstone (<http://mapapps.bgs.ac.uk/geologyofbritain/home.html>), which is overlaid by freely draining loamy soils (Soil Survey of England and Wales, 1983). Land use on the catchment plateaux is dominated by cropland in rotation of arable crops and temporary grassland (also referred to as grass ley), while permanent grassland is found on steeper hillslopes, with riparian vegetation (mostly wet woodland dominated by willow *Salix sp.*, alder *Alnus glutinosa* and wet grassland) located in the riparian zone within the river corridor.

2.2 Field sampling

78 soil cores were taken along 14 hillslope transects across the two sub-catchments (8 cm diameter, depth 0-15 cm), covering the topographic sequence from plateaux, convex, steep slope, concave and footslope locations. In total, 31 samples were taken from arable land use, 26 from temporary grassland (ley), 14 from permanent grassland and 7 from riparian woodland. Three river-bed sediment samples were collected with a hand trowel and bulked into a single sample on a single occasion at 7 locations along each of the two streams at an (i) upstream (ii) midstream and (iii) downstream location and the joint catchment outlet before the confluence with Loe Pool. Two 0.5 m deep lake sediment cores were taken from Loe Pool c. 150 m below the outlet of Carminowe Creek using a Mackereth corer (Mackereth, 1969).

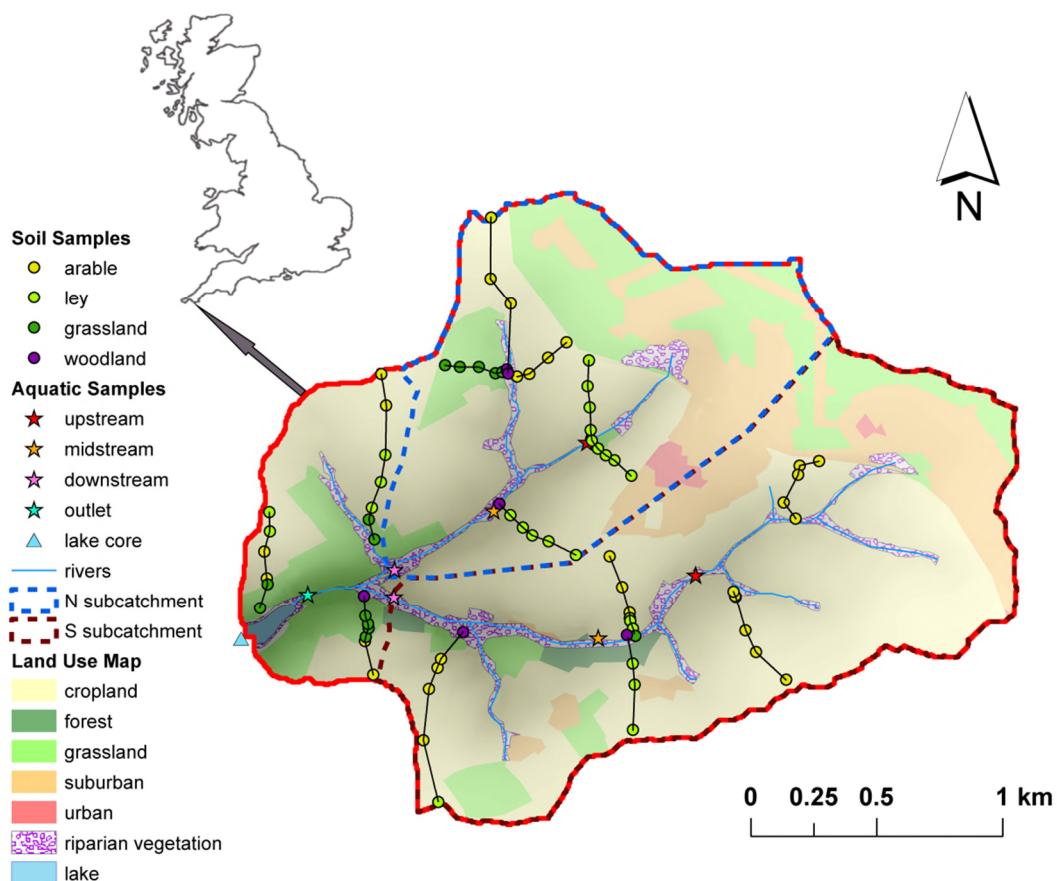


Fig. 1 The study site location in south-west England showing land use, the 14 study transects, river bed sediment sampling locations and the lake core.

2.3 Laboratory analysis

Following sample collection, river bed and lake core sediment samples were stored at 4°C and analysed as soon as possible. Soil samples were oven dried at 40°C and sieved to <2 mm and >2 mm fractions. River bed samples were wet sieved at 250 µm to separate coarse vegetation debris as in Galy et al. (2011) and the < 250 µm fraction was oven dried at 40°C and retained for further analysis. The lake sediment core was sliced into 2 cm increments and freeze dried.

All soil, river bed sediment and lake core samples were analysed for total C, N and bulk $\delta^{13}\text{C}$ and $\delta^{15}\text{N}$ using a SerCon Integra2 isotope ratio mass spectrometer (SerCon Ltd., Crewe, UK). An in house standard of Alanine (N=16.7%, C=40%, $\delta^{15}\text{N}=-1.68\text{‰}_{\text{AIR}}$, and $\delta^{13}\text{C}=-19.58\text{‰}_{\text{VPDB}}$) was used in duplicate every 9 samples to provide quality control and to act as an internal reference. This was calibrated within each analytical run by also analysing International Atomic Energy Agency (IAEA) reference materials N-1 and N-2 for nitrogen and CH-6 and LSVEC for carbon. Data was corrected for background signal by subtracting blank sample values and a linearity correction was applied based on the analysis of the IAEA reference materials. Analytical precision was determined by repeat measurement of quality control samples of alanine throughout the analytical run. Measurements of these samples had standard deviations of $<0.3\text{‰}$ and $<0.1\text{‰}$, respectively, for $\delta^{15}\text{N}$ and $\delta^{13}\text{C}$.

The values were expressed relative to AIR and Vienna PeeDee Belemnite (VPDB) for nitrogen and carbon respectively. The formula used for presenting δ values is as follows:

$$\delta^{15}\text{N X ‰}_{\text{AIR}} = (R_{\text{sam}}/R_{\text{ref}}-1)*1000 \quad (1)$$

$$\delta^{13}\text{C X ‰}_{\text{VPDB}} = (R_{\text{sam}}/R_{\text{ref}}-1)*1000 \quad (2)$$

Where sam is sample and ref is the reference material, R is the ratio of the heavy isotope over the light isotope, X being the isotope ratio expressed in units of per mille (‰).

In order to establish a chronology for the lake core profile, ^{137}Cs assay of individual 2 cm core sections was undertaken at 661.67 KeV using an ORTEC GMX co-axial HPGe γ -detector, coupled to a multi-channel analyser. Sample count times were generally 24 hours, resulting in analytical precision of c. 5%.

On the basis of likely hydrological connectivity with the watercourses, we selected a sub-set of 50 samples to estimate *n*-alkane concentrations ($\mu\text{g g}^{-1}\text{ C}$) from soil samples. Lake core samples were combined into 4 cm increments. The procedure of total lipid extraction was followed by lipid fractionation to isolate the hydrocarbon fraction for analysis using an Agilent 6890 GC instrument coupled to an Agilent 5973 MS instrument and equipped with an Agilent DB-5 ms column (30 m x 250 μm i.d.x 0.25 μm film thickness). The dominant fragment ions (base peak) were represented by m/z 57 and the diagnostic ions (m/z) 282 (C_{20}), 296 (C_{21}), 324 (C_{23}), 338 (C_{24}), 352 (C_{25}), 366 (C_{26}), 380 (C_{27}), 394 (C_{28}), 408 (C_{29}), 422 (C_{30}), 436 (C_{31}), 450 (C_{32}), 464 (C_{33}) and 478 (C_{34} , internal standard) (Norris, 2013). The concentrations of individual *n*-alkanes were determined relative to the C_{34} internal standard.

Interpretation of *n*-alkane results used the percentage of C_{27} , C_{29} and C_{31} calculated as (Torres et al., 2014):

$$\% \text{C}_i = \text{C}_i / (\text{C}_{27} + \text{C}_{29} + \text{C}_{31}) \quad (3)$$

where C_i stands for the respective *n*-alkane (C_{27} , C_{29} and C_{31}).

We used the ratio between the shorter chain C_{27} (indicative of woody source (Zech et al., 2009) and longer chain C_{31} (indicative of grass source (Eckmeier and Wiesenberg, 2009) to

distinguish between respective contributions of OM from woodland and grassland land uses (Puttock et al., 2014).

2.4 Indicators of aquatic versus terrestrial OM sources

To interpret the relative contribution of higher aquatic vs. terrestrial plants to OM in river and lake sediments we used the following formula (Ficken et al., 2000):

$$PAQ = \frac{(C_{23}+C_{25})}{(C_{23}+C_{25}+C_{29}+C_{31})} \quad (4)$$

where PAQ is the ratio of shorter-chain *n*-alkanes ($C_{23}+C_{25}$) contributed by higher aquatic plants (macrophytes) and mosses to the concentration (in $\mu\text{g g}^{-1}$) of *n*-alkanes indicative of both aquatic and terrestrial vegetation ($C_{23}+C_{25}+C_{29}+C_{31}$).

The proportion of OM from terrestrial sources in river bed sediments and in the lake core was calculated using the following formula (Fang et al., 2014; Meyers, 2003)

$$TAR = \frac{(C_{27}+C_{29}+C_{31})}{(C_{15}+C_{17}+C_{19})} \quad (5)$$

where TAR is terrestrial/aquatic ratio of the concentration of *n*-alkanes (in $\mu\text{g g}^{-1}$) derived from terrestrial sources ($C_{27}+C_{29}+C_{31}$) to those indicative of aquatic algae ($C_{15}+C_{17}+C_{19}$).

Organic matter degradation in the lake core was examined using the odd-over-even predominance (OEP) *n*-alkane ratio (Zech et al., 2013) as follows:

$$OEP = (nC_{27} + nC_{29} + nC_{31} + nC_{33}) / (nC_{28} + nC_{30} + nC_{32}) \quad (6)$$

High OEPs point either to an increased OM input and/or to an increased OM preservation while low OEPs are indicative of accelerated degradation under aerobic conditions (Zech et al., 2013).

We used $\delta^{13}\text{C}$, $\delta^{15}\text{N}$ and C/N ratio as further geochemical proxies to understand the proportion of OM contributed by algal vs. terrestrial plant derived production as used in previous studies (Fang et al., 2014; Hamilton and Lewis, 1992; Meyers, 2003).

2.5 Statistical Analysis

OM provenance was examined as follows. Firstly, Kruskal-Wallis non-parametric test was used to examine the differences between elemental (C/N) and isotopic ($\delta^{15}\text{N}$, $\delta^{13}\text{C}$) signatures between different sediment sources. All soil, river bed sediment and lake core increments were included in this analysis. Principal component analysis (PCA) was then used to examine whether elemental and *n*-alkane ratios could distinguish the provenance of OM derived from six potential sources (arable, temporary grassland (ley), permanent grassland, riparian woodland, lake or river bed) (Appendix 1). Finally, OM source apportionment was modelled

using the Bayesian isotope mixing model for Stable Isotope Analysis in R (SIAR)' (Parnell and Jackson, 2008, R Core Team, 2014). All statistical analyses were undertaken in 'R' vs. 3.4.0.

3. Results & Discussion

3.1 Distinguishing between terrestrial and aquatic organic matter sources

Differences in OM characteristics between sources, based on elemental and stable isotopic ratios, were examined. The C/N ratio and bulk stable ^{13}C and ^{15}N isotopic signatures of the terrestrial soils, river bed sediments and lake core sediments were statistically significantly unique (Table 1, $p < 0.001$). Woodland and river bed sediments exhibited the highest C/N ratios, while the lowest C/N ratios were detected in arable and temporary grassland soils. The high C/N ratio in woodland soils and river sediments is characteristic of more recalcitrant OM sources such as wood, while the low C/N ratio is indicative of more decomposable OM with lower lignin content (Brady and Weil, 1999). Percentage C and % N were comparable between the woodland and grassland soils and lake sediments and differed from low % C and % N in cropland soils and river bed sediments, indicating fast OM turnover in cropland rotations and rapid loss of OM and inorganic N from river bed sediments to the downstream lake.

In terms of OM ^{13}C and ^{15}N isotopic signatures, the highest bulk $\delta^{15}\text{N}$ values were detected in lake core sediments, followed by grassland and arable soils. Enriched $\delta^{15}\text{N}$ values in lake sediments may be due to several processes, including significant macrophyte or riparian-aquatic OM inputs (Fang et al., 2014), increased denitrification in anoxic lake bottom waters, and increased net primary production (Meyers, 2003). Increased bulk $\delta^{15}\text{N}$ values on arable land may be indicative of both rapid turnover of OM and long-term application of manure (Glendell et al., 2014b). Bulk $\delta^{13}\text{C}$ values were relatively uniform between land uses, reflecting the predominance of C3 plants in the study catchment (Puttock et al., 2014). $\delta^{13}\text{C}$ values were enriched in arable soils and lake core sediments, with the former possibly reflecting periodic growing of maize, a C4 plant with a different photosynthetic pathway with natural abundance $\delta^{13}\text{C}$ values of $\sim -12\text{‰}$ (Beniston et al., 2015; Puttock et al., 2014) on arable land and the effect of in-lake organic matter production on lake bed sediments (Fang et al., 2014; Hamilton and Lewis, 1992). However, it is important to acknowledge that direct characterisation of the composition of autochthonous OM produced by aquatic plants in the lake ecosystem would allow a more conclusive interpretation of these findings.

Table 1 Elemental and isotopic composition (mean and SD in brackets) of all terrestrial soils, river bed sediment and lake core samples. Values followed by the same letter are not significantly different, while values followed by a different letter are significantly different ($p < 0.05$). N = number of replicates.

| Landuse (N) | C/N | $\delta^{15}\text{N}$ (‰) | $\delta^{13}\text{C}$ (‰) | % C | % N |
|-------------|--------------|---------------------------|---------------------------|--------------|--------------|
| Arable (31) | 8.99 (0.7) a | 5.5 (0.8) a | -27.6 (0.4) a | 2.92 (0.54)a | 0.32 (0.05)a |
| Grass (14) | 9.98 (0.8) b | 5.6 (1.2) a, c | -28.2 (0.5) b | 5.60 (1.21)b | 0.56 (0.14)b |

| | | | | | |
|--------------|---------------|----------------|----------------|--------------|---------------|
| Ley (26) | 9.23 (0.7) a | 5.5 (0.9) a, c | -28.2 (0.40) b | 3.60 (0.82)c | 0.39 (0.07)c |
| Woodland (7) | 12.84 (2.4) c | 4.7 (1.5) a, c | -28.2 (0.3) b | 8.06 (1.83)b | 0.63 (0.14)bd |
| River (7) | 12.20 (1.0) c | 4.5 (1.1) a, d | -28.3 (0.2) b | 2.34 (0.84)a | 0.19 (0.06)a |
| Lake (27) | 10.76 (0.6) c | 6.3 (0.4) b | -27.6 (0.4) a | 7.40 (1.08)b | 0.69 (0.07)d |

Concentrations of *n*-alkanes of chain lengths C₁₅-C₃₃ in the six environments of interest showed a higher concentration of woody- (C₂₇-C₂₉) and grass- (C₃₁) derived OM input in lake sediments, as compared to terrestrial soils. Concurrently, shorter-chain *n*-alkanes indicative of aquatic macrophytes and lower plants such as mosses (C₂₁-C₂₅) (Meyers, 2003) were also apparent in lake sediments and in riparian woodland (Table 2). As expected, C₃₁ chain lengths indicative of grasses (forage and cereals) (Eckmeier and Wiesenberg, 2009), were more abundant in the soils of arable, ley and permanent grassland land uses, while the C₂₇ chain-length *n*-alkanes, indicative of woody vegetation (Zech et al., 2009), were more abundant in woodland soils, river bed and lake core sediments.

Table 2 *n*-alkane concentrations (µg g⁻¹ C) in soils and sediments from the six target environments. N – number of replicates.

| N | n-alkane chain length concentration µg g ⁻¹ C | | | | | | | | | |
|--------------|--|-------------|-------------|-------------|-------------|-------------|--------------|--------------|--------------|-------------|
| | Mean (SD) | | | | | | | | | |
| Landuse | C15 | C17 | C19 | C21 | C23 | C25 | C27 | C29 | C31 | C33 |
| Arable (11) | 0.16 (0.11) | 0.22 (0.12) | n/a | 0.65 (0.73) | 0.22 (0.11) | 0.40 (0.12) | 0.93 (0.34) | 2.68 (1.27) | 3.86 (0.91) | 1.99 (0.48) |
| Grass (7) | 0.26 (0.18) | 0.26 (0.17) | n/a | 0.43 (0.17) | 0.35 (0.20) | 0.76 (0.33) | 1.86 (1.32) | 3.81 (1.32) | 5.52 (1.25) | 3.02 (1.02) |
| Ley (9) | 0.25 (0.25) | 0.32 (0.29) | n/a | 0.92 (0.98) | 0.46 (0.70) | 0.83 (0.79) | 1.29 (0.74) | 3.10 (1.09) | 4.79 (1.46) | 2.22 (0.91) |
| Woodland (4) | 0.11 (0.13) | 0.22 (0.24) | n/a | 0.94 (0.86) | 0.92 (0.69) | 2.98 (1.09) | 12.93 (6.29) | 13.89 (5.09) | 7.40 (2.86) | 4.40 (2.61) |
| River (7) | 0.24 (0.20) | 0.24 (0.21) | 0.22 (0.09) | 0.46 (0.40) | 0.37 (0.20) | 1.35 (0.51) | 5.70 (2.11) | 5.92 (2.24) | 2.65 (1.04) | 1.10 (0.52) |
| Lake (12) | 0.26 (0.18) | 1.28 (0.85) | 0.96 (0.42) | 0.96 (0.43) | 1.90 (0.70) | 4.17 (1.42) | 16.45 (4.27) | 16.62 (2.91) | 12.08 (1.55) | 4.93 (1.23) |

Relative contribution of aquatic vs. terrestrial plants to OM was assessed with three indicators, C₂₇/C₃₁ ratios, PAQ and TAR. As expected highest C₂₇/C₃₁ ratios, indicative of woody sources were found in the woodland soil samples, while low C₂₇/C₃₁ ratios in the remaining terrestrial soils were indicative of OM origin from grassland vegetation (including cereal crops and forage grass). The river bed sediments were also characterised by higher C₂₇/C₃₁ ratios, indicating predominant sediment input from soils under woody vegetation in the well-connected wooded riparian buffer strip (Fig. 2a). The lake sediments appear to be intermediary between these land uses, indicating OM contribution from both woody and grass vegetation, which may be related to OM transport during high-flow events. During rainfall events, the otherwise less connected

arable/grassland sources may make a greater contribution to OM transport, which is likely to be directly routed to the lake, without being deposited in river bed sediments.

Higher median PAQ ratios of > 0.15 in the lake, river and riparian woodland environments were indicative of emergent macrophyte origin, while the lower median ratios < 0.1 were indicative of terrestrial plants (Fig. 2b). The higher PAQ ratios in the riparian woodland may reflect a contribution from lower plants including mosses, which were abundant on the ground of this wet woodland. Still there remains a large unexplained variability of observed PAQ, particularly in the grass ley.

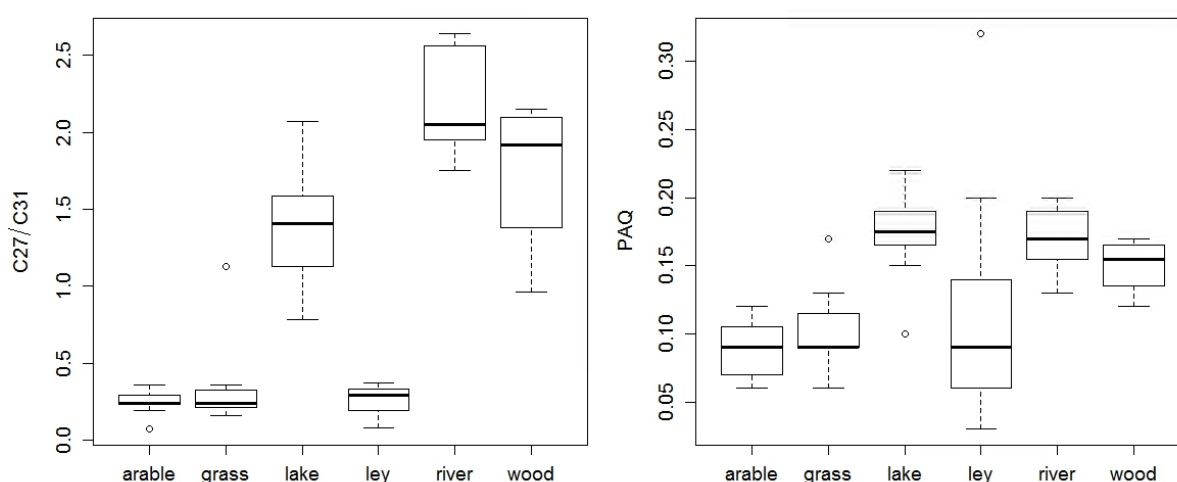


Fig. 2 Box plots of *n*-alkane ratios a) C_{27}/C_{31} indicating OM prevalence from woody vs. grass dominated sources b) PAQ indicating contribution of OM from aquatic/lower plant vs. terrestrial vegetation. The bottom and top of the box refer to the 25th and 75th percentile, the bold line near the middle to the 50th percentile (the median) and whiskers represent the smallest and largest values within 1.5 times of the interquartile range (i.e. the distance between the 25th and 75th percentile). Any data outside of whiskers are represented as outliers as they exceed 1.5 times of the interquartile range.

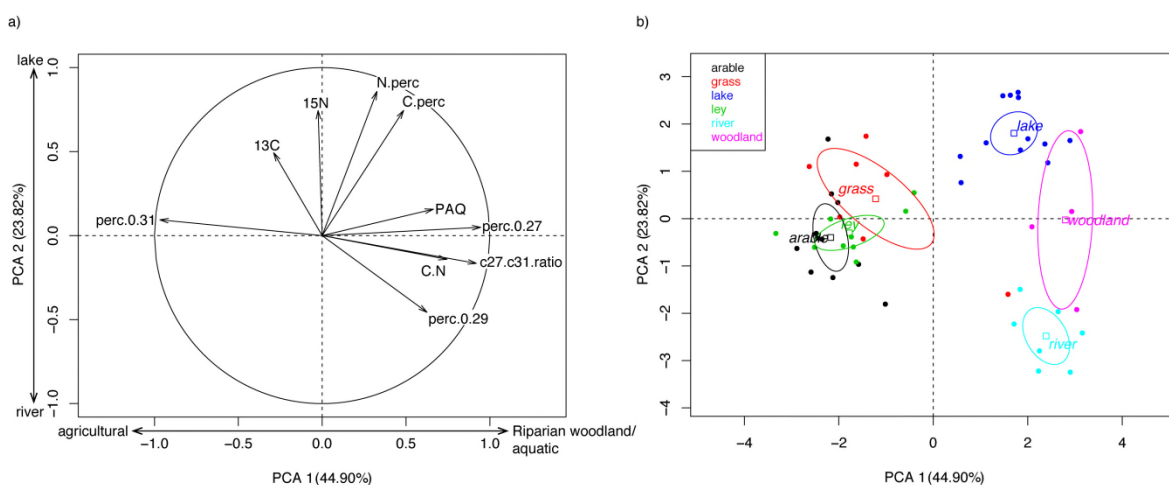
While single tracers and ratios presented above cannot unravel contribution of several sources on their own, a global assessment with a Principal Component Analysis (PCA) was undertaken. PCA revealed that a combined *n*-alkane, elemental and stable ^{13}C and ^{15}N isotopic signatures provide a clear separation in sediment fingerprint composition (Fig. 3). The PCA axis 1 can be interpreted as a gradient between grassland and arable land uses with higher % C_{31} *n*-alkane signature (indicating grass-derived OM) vs. riparian woodland and aquatic environments with a higher % C_{27} , higher $C_{27}:C_{31}$ and C/N ratios (indicating wood-derived OM sources), lower % C_{29} (indicating lower plants in the woodland ground vegetation) and higher PAQ (Tables 1-3, Fig. 3a). The PCA axis 2 can be interpreted as a gradient between river bed sediments and lake core sediments, with the latter supporting higher $\delta^{13}C$ and $\delta^{15}N$ isotopic signatures and higher % C and % N content (Tables 1-3, Fig. 3a) and indicating different sediment dynamics in the two aquatic environments. This is also reflected in Fig 3b, which shows a clear distinction in

sediment composition between lake and river bed sediments and woodland, permanent grassland and cropland sources. PCA axis 3 accounts for a further 10.65 % of variance and may help to discern between terrestrial (riparian woodland and grassland) vs. river-bed OM sources, with the latter supporting a higher PAQ ratio, lower $\delta^{15}\text{N}$, lower % C and lower % N (Fig.2b, Table 1), possibly reflecting in-stream OM production. However, PCA could not distinguish soils from temporary grassland (ley) and arable land, presumably because these two land uses are subject to regular rotations. While other researchers have also found it possible to distinguish between permanent grassland and woodland sediment and OM sources, they were unable to distinguish between arable land use and permanent grassland, based on the use of biomarkers alone (Alewell et al., 2015). In this study, the combined use of biomarkers and elements (% C, % N, C/N ratio) allowed us to distinguish between these two land uses as the % N and % C as well as C/N ratio are all higher in grassland soils than in arable and temporary grass ley (Appendix 1, Table 3), thus acting as further informative tracers in addition to *n*-alkanes.

Table 3 Loading scores of ten biochemical tracers, initial eigenvalues and % total variance accounted for by the first three PCA axes with eigenvalues >1. Loading scores >0.3 were used in the interpretation of axes.

| | axis 1 | axis 2 | axis 3 |
|-----------|--------|--------|--------|
| %N | 0.33 | 0.86 | -0.34 |
| delta 15N | | 0.74 | 0.48 |
| %C | 0.49 | 0.75 | -0.45 |
| C/N | 0.74 | | -0.38 |
| delta 13C | | 0.49 | 0.34 |
| C27/C31 | 0.92 | | |
| PAQ | 0.66 | | 0.35 |
| C27 | 0.95 | | |
| C29 | 0.63 | -0.46 | |
| C31 | -0.97 | | |
| Arable | -2.17 | -0.40 | |
| Grass | -1.22 | 0.42 | -0.81 |
| Lake | 1.71 | 1.80 | |
| Ley | -1.77 | | |

| | | | |
|--------------------------|-------|-------|-------|
| River | 2.39 | -2.48 | 0.91 |
| woodland | 2.79 | | -1.28 |
| Eigenvalues | 4.49 | 2.38 | 1.06 |
| % of variance | 44.90 | 23.82 | 10.65 |
| Cumulative % of variance | 44.90 | 68.71 | 79.36 |

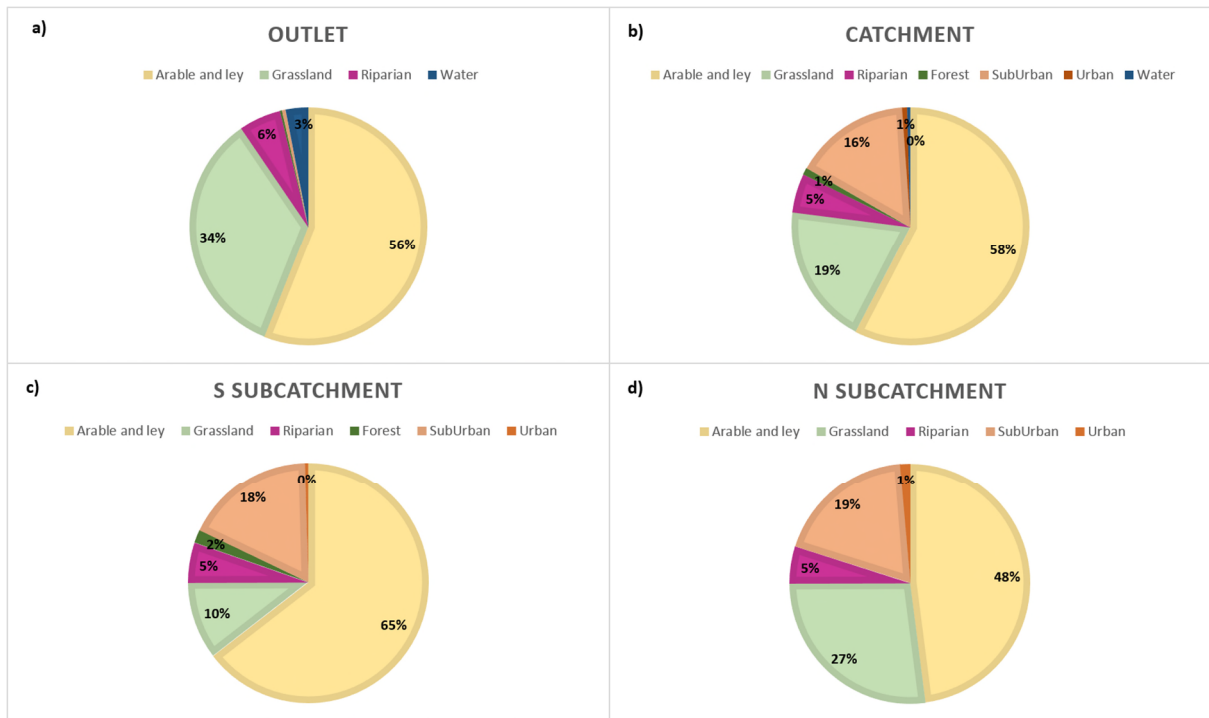


1
2 Fig. 3 Two-dimensional plot of a) variable distribution along the first two PCA ordination axes
3 b) sampling site loading scores on the first two PCA axes and 95% confidence ellipses around
4 the categories of land use.

5 3.2 Spatial variability of land use and provenance of OM in river bed sediments

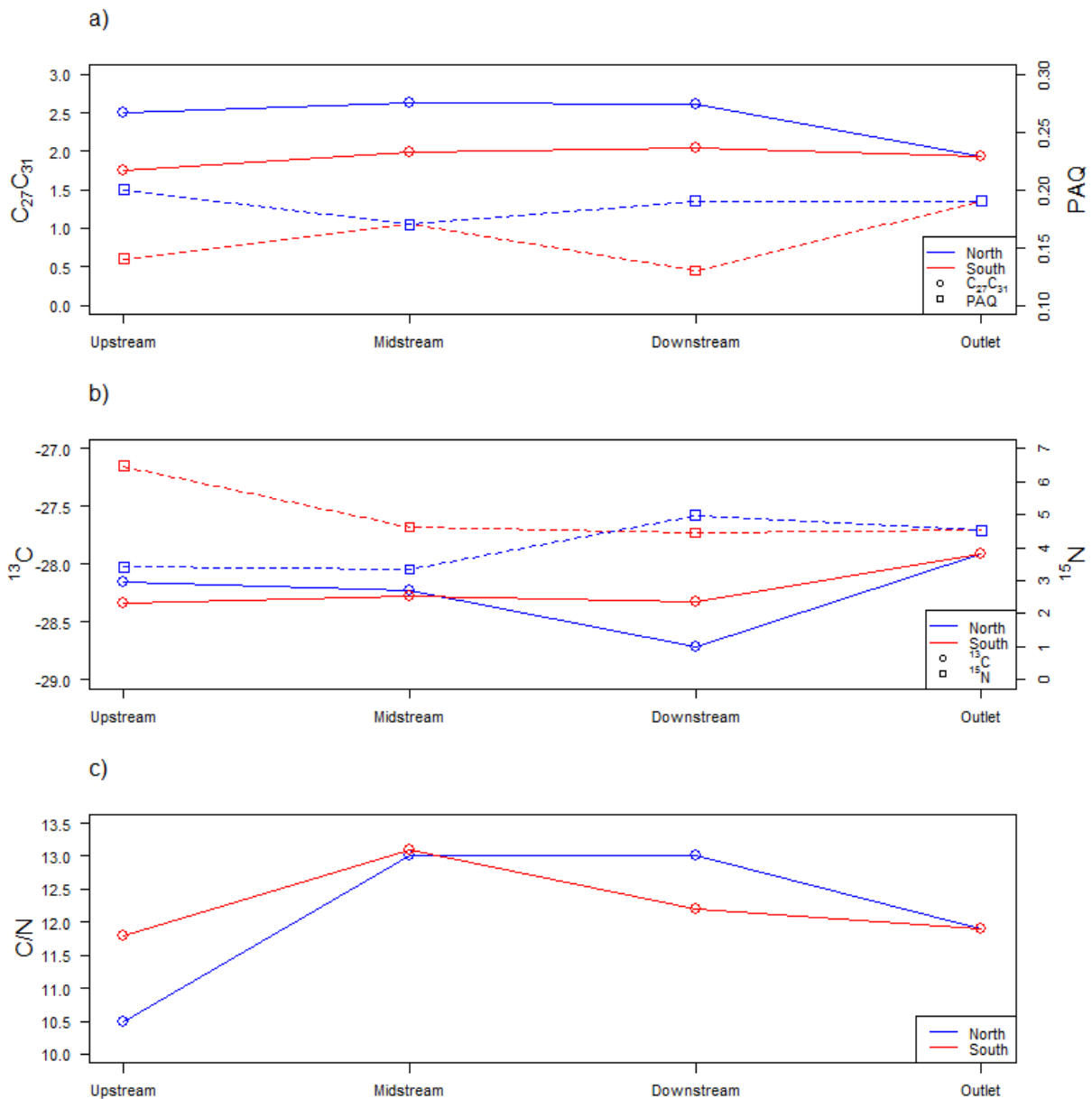
6 Spatial patterns of OM provenance in relation to land use were examined at each river bed
7 sediment sampling location (“upstream”, midstream”, “downstream” and “outlet”) in the two
8 subcatchments (S and N) (Figs. 1, 4, 5). Organic matter fingerprinting properties reflected some
9 subtle differences in land used between the two subcatchments. While both the S and N
10 subcatchments were characterized by ca. 75 % agricultural land use, 20 % sub-urban land use
11 and 5 % of riparian vegetation in the riparian corridor, the S subcatchment supported a higher
12 arable and ley vs. permanent grassland ratio (65 % to 10 %, respectively) than the N
13 subcatchment (48 % to 19 %, respectively) (Fig. 4).

14



15

16 Fig. 4 Proportion of different land uses a) at the outlet sampling location b) the whole study
 17 catchment c) Southern subcatchment and d) Northern subcatchment.



18

19 Fig. 5 Spatial variability of a) *n*-alkane proxies b) stable isotopes and c) C/N ratio in a
 20 downstream direction in the two subcatchments. Each data point at upstream, midstream and
 21 downstream location and the catchment outlet represents a composite of three individual river-
 22 bed sediment samples.

23 This was reflected in river bed OM properties, which had remarkably lower C_{27}/C_{31} ratios (1-
 24 0.5) in the S subcatchment than in the N subcatchment, with the upstream location supporting
 25 the lowest C_{27}/C_{31} *n*-alkane value of 1.75 overall (Fig 5a), likely due to a higher proportion of
 26 arable and ley land use at this location (Fig 4c) leading to higher soil erosion rates (Turnage et
 27 al., 1997) and a higher contribution from C_{31} dominated sources (e.g. wheat, ley). The observed
 28 higher $\delta^{15}N$ values at the most upstream location in the S subcatchment (ca.+7 ‰, Fig 5b) may
 29 also be associated with a higher application of farmyard manure and slurry on the arable land
 30 and ley in this part of the catchment (Bol et al., 2005; Senbayram et al., 2008). Conversely, the
 31 higher C_{27}/C_{31} ratio in the N subcatchment and the lack of upstream forested areas indicate a

32 higher contribution of OM from wooded vegetation in the riparian zone, as well as a potential
33 buffering of terrestrial OM fluxes from agricultural soils in this vegetated river corridor.
34 Although the within-subcatchment variability in PAQ ratio tend to be rather large, it can be
35 hypothesised that overall the higher PAQ ratios in the N subcatchment indicate a relatively
36 higher contribution of mosses and macrophytes derived OM and point towards a greater
37 influence of the riparian zone on lateral C fluxes in the N stream as compared to the S stream
38 (Fig. 5a).

39 Higher C_{27}/C_{31} and C/N ratios (Fig. 5a & 5c) at the midstream and downstream locations in
40 both subcatchments indicated an increased contribution of OM from woody vegetation to river
41 bed sediments in these river reaches. The C_{27}/C_{31} *n*-alkane ratio at the joint catchment outlet
42 was lower than in the N subcatchment but similar to the ratios found in the S subcatchment
43 (Fig. 5a), indicating mixing of OM from the two tributaries as well as input from permanent
44 grasslands situated on the steep slopes in the lower reaches of the river corridor. No remarkable
45 difference in ^{13}C between N and S subcatchment could be detected, except some slightly higher
46 values at the outlet location, which may indicate some enhanced decomposition of OM at these
47 locations. Nevertheless, a more refined sampling strategy, including the analysis of replicate
48 samples instead of their composites, may allow a more detailed characterisation of the spatial
49 variability of the studied biochemical proxies and a stronger statistical interpretation of the
50 influence of land use, agro-management and/or topographical differences within the catchment
51 on the spatial variability of lateral C fluxes.

52

53 3.3 Impact of land use on sediment and C accumulation in lake bed sediments

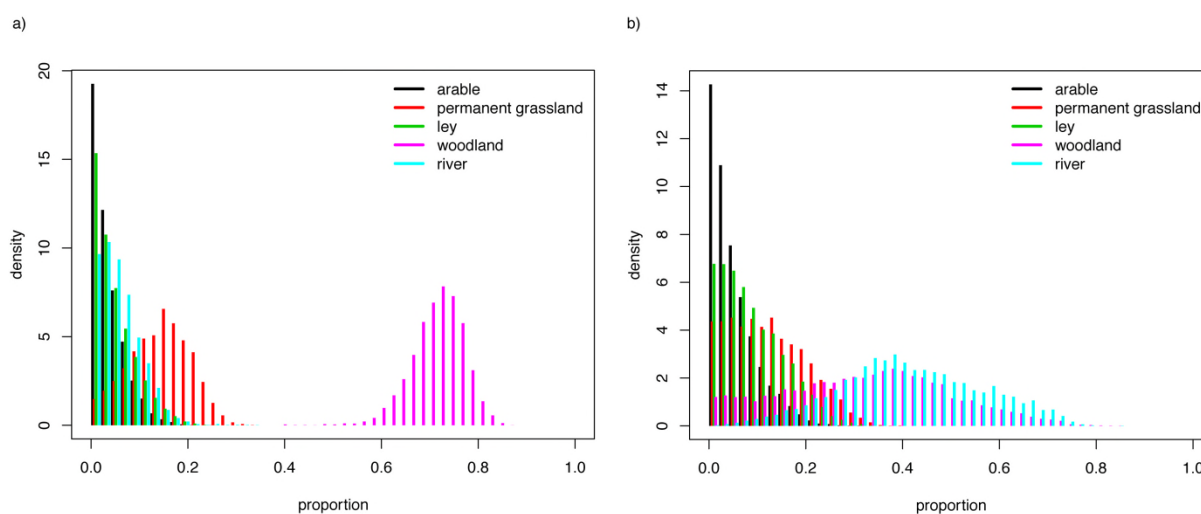
54

55 Source apportionment modelling of the lake core sediments has shown different results,
56 depending on the number of tracers included in the mixing model. Currently, there is a lack of
57 consensus within the sediment fingerprinting community on the most appropriate selection of
58 fingerprint tracers (Sherriff et al., 2015; Zhang and Liu, 2016). Therefore, in this study, we
59 firstly included all tracers used in the PCA in the source apportionment analysis (Fig. 6a),
60 followed by just those tracers that encompassed the range of values represented in the mixture
61 (and were therefore deemed as conservative) (Fig. 6b). The second approach included $C_{27}:C_{31}$
62 ratio, % C_{27} , % C_{29} and % C_{31} . As such we had 4 tracers (n) to apportion the contribution of
63 five sources (n+1). In both cases, organic C from riparian woodland was a major contributor
64 to the lake sediments. In the second scenario, river bed sediments also appeared to make an
65 important contribution to lake sediments over the past 60 years, comparable to that derived
66 from woodland (Fig. 6b). However, as river bed sediments are also dominated by woody
67 vegetation, as shown in Fig. 2a above, they can be considered 'equal to' woodland signatures
68 in this apportionment model, due to the restricted number of very selective tracers. However,
69 in both modelling outcomes, the important contribution of organic matter from permanent
70 grassland, which occupies the steep slopes surrounding the lake, is very apparent (Fig. 6a).

71 Zhang and Liu (2016) also found that tracer selection greatly impacted the estimated source
72 contributions, due to a number of potential reasons, including i) tracer conflicts ii) tracer
73 measurement error and iii) differences in tracer conservativeness. Therefore, they proposed to
74 use multiple fingerprints to derive ‘average’ estimated source contribution proportions, instead
75 of just a single fingerprint set. While different sediment contributions can be obtained with
76 different fingerprint selection, recent studies (Palazón et al., 2015; Sherriff et al., 2015) have
77 found that inclusion of more tracers improved the source apportionment results. In this study,
78 modelling results based on the full set of tracers (Fig. 6a) allowed a finer distinction between
79 contributing land uses.

80

81 Conversely to lake core sediments, it was not possible to model the source apportionment of
82 river bed sediments satisfactorily as all potential tracers in bed sediments appeared to be outside
83 the range of the potential sources. This apparently ‘missing source’ opens new lines of enquiry
84 for future research. At present we hypothesise that the ‘missing source’ may either be due to
85 the contribution of petrogenic C originating from the underlying bedrock (Galy et al., 2015) or
86 that the *n*-alkane signatures have been altered by autochthonous in-stream production of OM
87 (e.g. from algae) and by in-stream biological processing of river bed sediments (Chen et al.,
88 2016).



1
2 Fig. 6 Probability density function of sediment source apportionment sources from different
3 land uses using a) all available tracers b) only tracers that encompass the full range of values
4 present in the mixture for the application of the mixing model SIAR.

5

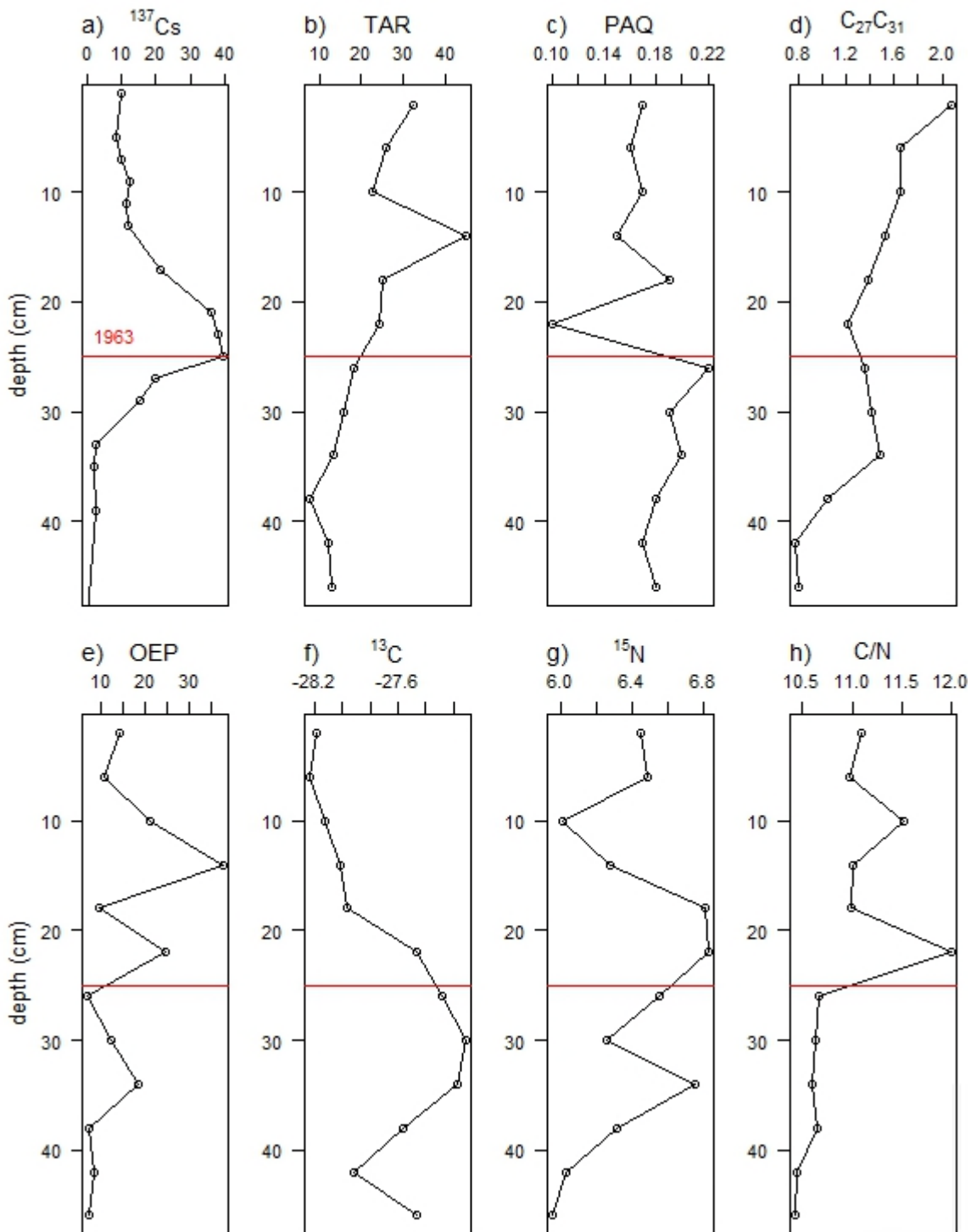
6 3.4 Understanding the temporal variability of lateral C fluxes from land to water in relation 7 to land use change

8

9 Caesium-137 (^{137}Cs) activity was used to get an approximate dating profile for the lake bed
 10 sediment core (Fig. 7a). The depth distribution of ^{137}Cs within the core was analysed and the
 11 horizon containing peak activity was identified at 26 cm and was assumed to be associated with
 12 the peak in bomb derived ^{137}Cs fallout attributed to 1963. The offset of bomb testing in 1952
 13 was assumed to be associated with lake core depth at 34 cm.

14

15



16

17 Figure 7 Lake core profiles showing a) ^{137}Cs activity used to date the lake sediment core and
18 interpret the observed changes in sediment composition over time b-h) sediment fingerprinting
19 characteristics with depth.

20

21 The combined use of *n*-alkane ratios and stable isotope signatures shows a variable contribution
22 of terrestrial *vs.* aquatic sources to sediment accumulation in individual lake core increments
23 over the past 60 years (Fig. 7b-h). As the lake core was taken relatively close to the river outlet
24 (Fig. 1), this part of the lake environment is likely to be characterized by high deposition rates
25 of terrestrial derived sediments and OM from the fluvial system. This may explain why the
26 range of TAR ratio values found in this study (i.e. 10 – 40, Fig. 7b) was higher than in
27 comparable studies elsewhere (e.g. values between: 1 and 5 in lakes Ontario and Erie
28 (Bourbonniere and Meyers, 1996); 2 and 10 in lake Tianyang in South China (Wang et al.,
29 2014), which mostly considered cores in the middle of larger lakes with the specific aim to
30 detect paleoclimatological variations. Furthermore, the overall increasing trend in TAR
31 indicates an increasing contribution of terrestrial-derived OM to the lake sediments over time,
32 while the increasing $\text{C}_{27}/\text{C}_{31}$ ratio (Fig. 7d) indicates an increase of woody vegetation
33 contribution over the same time period. This is corroborated by the fact that the signal from
34 PAQ *n*-alkane proxy lies within the range of 0.01 to 0.23 (Fig. 7c), deemed indicative of
35 terrestrial plants (Silliman and Schelske, 2003) and suggesting mainly allochthonous source of
36 sedimentary OM. The depletion in $\delta^{13}\text{C}$ values with depth (Fig. 7f) may also indicate an
37 increasing input of isotopically lighter soil-derived dissolved inorganic C (Meyers, 2003) – and
38 thus increasing terrestrial input of C from soil erosion. However, it may also be due to the
39 preferential loss of the light isotope (^{12}C) through microbial respiration over time (Beniston,
40 et al. 2014). In any case correlation between OEP and TAR ratios ($p < 0.001$, $R^2 = 0.53$) suggests
41 reduced OM decomposition associated with increasing terrestrial contribution of OM over the
42 past 60 years (Zech et al., 2013), which may be linked to a higher C/N ratio – and therefore
43 lower bioavailability of woodland and grassland derived OM.

44 Overall the observed $\delta^{15}\text{N}$ values in Loe Pool lake sediment samples within the range of 6 to
45 6.8 ‰ (Fig. 7g) are rather high when compared to other studies (e.g. reporting values between:
46 -1‰ and +6‰ across a wide range of lakes in Florida (Brenner et al., 1999); +3‰ and +6‰
47 for Lake Baikal (Yoshii et al., 1997); +6‰ and +8‰ for lake Qinghai in Tibet (Xu et al., 2006);
48 +3‰ and +8‰ for lake Ontario (Hodell and Schelske, 1998)), which can be explained by likely
49 higher inputs of organic nutrients from agricultural run-off, from two sewage treatment plants
50 located within the study catchment and the observed associated eutrophication of the lake since
51 the 1960s (National Trust, 2017). Despite this limited range in $\delta^{15}\text{N}$ values and the rather large
52 variability throughout the entire core, the middle section of the core is characterized by
53 noticeably higher $\delta^{15}\text{N}$ values, particularly during the period shortly after 1963 (around 20 cm
54 depth in the lake core). This may be indicative of increased net primary production (NPP)
55 associated with the reported eutrophication of Loe Pool since the 1960s (Dinsdale, 2009) but
56 is not likely to be due to an increase in N fixing cyanobacteria, which directly fix atmospheric
57 N_2 and therefore lead to lower $\delta^{15}\text{N}$ signatures in sediments and would be expected to lead to

58 an increased $\delta^{13}\text{C}$ signature due to enhanced NPP (Meyers and Lallier-Vergès, 1999; Meyers,
59 2003). In addition, increased $\delta^{15}\text{N}$ enrichment may be associated with enhanced denitrification
60 (preferential loss of the light ^{14}N isotope) in anoxic lake bottom waters (Meyers, 2003) or with
61 higher natural abundance ^{15}N -enriched signatures originating from faeces from farmyard
62 manures (Senbayram et al. 2008) and septic tanks (Collins, et al. 2013; 2014). These higher
63 ^{15}N values shortly after 1963 coincide with a peak in C/N ratio, decreasing PAQ and increasing
64 TAR, which provides further evidence of increased OM input from terrestrial sources as a
65 likely consequence of intensive agricultural practices and associated higher erosion rates during
66 the 1960-1980's. Conversely, in the uppermost depth increments (ca. top 12 cm), representing
67 more recent sediment depositions, these relationships seems to gradually disappear and/or
68 proxy values tend to return to their pre-1960's levels. This may coincide with lake remediation
69 measures introduced by the landowner (The National Trust) since 1996 through targeted agro-
70 management interventions to reduce the amount of fertilizer and organic manure applied on the
71 arable land within the catchment (National Trust, 2017; Loe Pool Forum, 2017).

72

73 However, it is acknowledged that $\delta^{13}\text{C}$ enrichment and C/N ratios are not always indicative of
74 sources as they can be affected by degradation (Ranjan et al., 2015). Lacey et al. (2015) found
75 that while $\delta^{15}\text{N}$ bulk isotopic signatures of sediment sources exhibited non-conservative
76 behaviour, $\delta^{13}\text{C}$ signatures appeared to be more stable. Fang et al. (2014) observed that
77 significant macrophyte or riparian-aquatic OM inputs may lead to higher $\delta^{15}\text{N}$ and $\delta^{13}\text{C}$ values
78 in lake sediments, thus confounding our ability to distinguish between the terrestrial and
79 aquatic input of OM on the basis of bulk stable ^{13}C and ^{15}N isotopic signatures alone. Therefore,
80 compound-specific stable ^{13}C isotope (CSSIA) signatures of plant-derived biomarkers are
81 currently explored as more suitable tracers, as the isotopic signatures of individual molecules
82 are likely to be more conservative than bulk stable isotopes alone (Fang et al., 2014; Tao et al.,
83 2016).

84 In this study, the combined use of *n*-alkanes and bulk stable ^{13}C and ^{15}N isotopes detected
85 increased terrestrial input of sediment and increased lake eutrophication over the past 60 years,
86 with terrestrial grass and woody plant-derived *n*-alkanes being more indicative of OM sources,
87 and stable ^{13}C and ^{15}N isotopes being more indicative of in-stream and in-lake processes. The
88 application of compound-specific stable isotope $\delta^{13}\text{C}$ and $\delta^2\text{H}$ signatures of specific *n*-alkane
89 molecules, as opposed to a separate use of *n*-alkane chain length and bulk stable ^{13}C and ^{15}N
90 isotopes, may help to better differential between aquatic and terrestrial plant origin of organic
91 matter in future work (Cooper et al., 2015) and thus quantify the autochthonous vs. allochthonous
92 organic matter contribution. Further improvements may be obtained by multi-molecular
93 investigations using simultaneous application of different biomarkers and ^{14}C isotopes to
94 constrain the transfer of C from land to the ocean (Feng et al., 2015).

95 The ability to discern OM contribution to aquatic environments from different land uses found
96 in this study, provides an important new tool for the understanding of OM fluxes from land to
97 water at catchment scales. Wohl et al. (2017) proposed a revised paradigm for the
98 understanding of the role of rivers in the transport and processing of terrestrial C, whereby the

99 active river channel and the riparian zone function as one coupled system – a *river corridor*, in
100 which riparian areas act ‘as biogeochemical reactors that facilitate the speciation,
101 transformation, and opportunities for both long-term storage of carbon and mineralization to
102 the atmosphere’. Wohl et al. (2017) posit that while alteration of riparian zone is the most
103 significant and most highly altered aspect of lateral C dynamics, very little is known about the
104 sources and quantities of different kinds of OM stored within river corridors and how C inputs
105 have varied over decadal and millennial timescales as a results of human activities. In this
106 study, we also found very close coupling between the aquatic sediments and the riparian zone
107 and our ability to discern between these sources provides a new opportunity to quantify the
108 lateral C fluxes at catchment scales. Coupling the fingerprinting approach explored in this
109 paper with future modelling of soil erosion rates is a promising new tool for quantifying these
110 lateral C fluxes at a range of scales.

111

112 **4. Conclusions**

113 This pilot study tested a new approach to quantify the lateral fluxes of OM from the terrestrial
114 to aquatic environments at a catchment scale. Here we evaluated the combined use of the
115 abundance and ratios of conservative plant-derived biomarkers *n*-alkanes and bulk stable
116 isotopes to distinguish between OM and sediment provenance from different environments.
117 While it was possible to distinguish between arable and temporary grassland vs. permanent
118 grassland vs. woodland vs. river vs. lake environments, it was not possible to distinguish
119 between arable land and temporary grassland, as these two land uses are part of regular
120 rotations. However, the combined use of biomarkers and stable isotopes allowed us to
121 distinguish between sediment sources from arable vs. permanent grassland land uses, which
122 has not been previously possible with the use of plant-derived biomarkers alone. Furthermore,
123 the combined use of biomarkers and stable isotopes enabled us to detect the observed change
124 in the lake trophic status over the past 60 years and attribute this to changing land use, resulting
125 in enhanced sedimentation and nutrient flux from the terrestrial to the aquatic environments.
126 These enhanced lateral OM fluxes can be linked to agricultural intensification, resulting in
127 higher soil erosion rates, over the same period. Moreover, we detected an increased
128 contribution of woody vegetation to the OM provenance over time, most likely indicating an
129 increase in the woody vegetation covering the near-stream riparian corridor. The new
130 fingerprinting approach successfully discriminated between terrestrial vs. aquatic C sources
131 and when coupled with quantitative estimates of soil erosion rates, it shows to be a promising
132 new tool for the understanding of lateral C fluxes from land to water at a range of scales. The
133 close coupling between OM provenance and riparian land use observed in this study underlines
134 the importance of the riparian zone for lateral C transfers and thus supports the new holistic
135 conceptualization of ‘river corridors’ as critical zones linking the terrestrial and aquatic C
136 cycles (Wohl et al., 2017).

137 **Acknowledgements** This work was supported by the University of Exeter Strategic Science
138 Development Fund and UK Natural Environment Research Council GW4+ Research
139 Experience Placement Scheme. We would like to thank Iain Hartley and Gabriel Yvon-

140 Durocher of the University of Exeter for helpful scientific discussions at the project inception
141 and to two anonymous reviewers for their constructive comments that greatly helped to
142 improve our manuscript.

143

144 **References**

145 Adhikari, K., Hartemink, A.E., 2016. Linking soils to ecosystem services - A global review.
146 *Geoderma* 262, 101–111. doi:10.1016/j.geoderma.2015.08.009

147 Alewell, C., Egli, M., Meusburger, K., 2015. An attempt to estimate tolerable soil erosion rates
148 by matching soil formation with denudation in Alpine grasslands. *J. Soils Sediments* 1–
149 17. doi:10.1007/s11368-014-0920-6

150 Alewell, C., Birkholz, A., Meusburger, K., Schindler Wildhaber, Y., Mabit, L., 2016.
151 Quantitative sediment source attribution with compound-specific isotope analysis in a C3
152 plant-dominated catchment (central Switzerland). *Biogeosciences* 13, 1587–1596.
153 doi:10.5194/bg-13-1587-2016

154 Alewell, C., Birkholz, A., Meusburger, K., Schindler Wildhaber, Y., Mabit, L., 2015. Sediment
155 source attribution from multiple land use systems with CSIA. *Biogeosciences Discuss.*
156 12, 14245–14269. doi:10.5194/bgd-12-14245-2015

157 Amundson, R., Berhe, A.A., Hopmans, J.W., Olson, C., Sztein, A.E., Sparks, D.L., 2015. Soil
158 science. Soil and human security in the 21st century. *Science* 348, 1261071.
159 doi:10.1126/science.1261071

160 Aufdenkampe, A.K., Mayorga, E., Raymond, P.A., Melack, J.M., Doney, S.C., Alin, S.R.,
161 Aalto, R.E., Yoo, K., 2011. Riverine coupling of biogeochemical cycles between land,
162 oceans, and atmosphere. *Front. Ecol. Environ.* 9, 53–60. doi:10.1890/100014

163 Battin, T.J., Luysaert, S., Kaplan, L. a., Aufdenkampe, A.K., Richter, A., Tranvik, L.J., 2009.
164 The boundless carbon cycle. *Nat. Geosci.* 2, 598–600. doi:10.1038/ngeo618

165 Beniston, J.W., DuPont, S.T., Glover, J.D., Lal, R., Dungait, J.A.J., 2014. Soil organic carbon
166 dynamics 75 years after land-use change in perennial grassland and annual wheat
167 agricultural systems. *Biogeochemistry* 120, 37–49.

168 Beniston, J.W., Shipitalo, M.J., Lal, R., Dayton, E.A., Hopkins, D.W., Jones, F., Joynes, A.,
169 Dungait, J.A.J., 2015. Carbon and macronutrient losses during accelerated erosion under
170 different tillage and residue management. *Eur. J. Soil Sci.* 66, 218–225.

171 Bilotta, G.S., Brazier, R.E., 2008. Understanding the influence of suspended solids on water
172 quality and aquatic biota. *Water Res.* 42, 2849–2861. doi:10.1016/j.watres.2008.03.018

173 Blake, W.H., Ficken, K.J., Taylor, P., Russell, M.A., Walling, D.E., 2012. Tracing crop-
174 specific sediment sources in agricultural catchments. *Geomorphology* 139–140, 322–329.
175 doi:10.1016/j.geomorph.2011.10.036

176 Bol, R., Eriksen, J., Smith, P., Garnett, M.H., Coleman, K., Christensen, B.T., 2005. The
177 natural abundance of ¹³C, ¹⁵N, ³⁴S and ¹⁴C in archived (1923-2000) plant and soil
178 samples from the Askov long-term experiments on animal manure and mineral fertilizer.

- 179 Rapid Commun. Mass Spectrom. 19, 3216–3226.
- 180 Bourbonniere, R.A., Meyers, P.A., 1996. Sedimentary geolipid records of historical changes
181 in the watersheds and productivities of Lakes Ontario and Erie. *Limnol. Oceanogr.* 41,
182 352–359. doi:10.4319/lo.1996.41.2.0352
- 183 Brady, N.C., Weil, R.R., 1999. *The Nature and Properties of Soils*. Prentice Hall, Upper Saddle
184 River, New Jersey.
- 185 Brenner, M., Whitmore, T.J., Curtis, J.H., Hodell, D.A., Schelske, C.L., 1999. Stable isotope
186 ($\delta^{13}\text{C}$ and $\delta^{15}\text{N}$) signatures of sedimented organic matter as indicators of historic lake
187 trophic state. *J. Paleolimnol.* 22, 205–221. doi:10.1023/A:1008078222806
- 188 Brevik, E.C., Cerdà, a., Mataix-Solera, J., Pereg, L., Quinton, J.N., Six, J., Van Oost, K., 2015.
189 The interdisciplinary nature of *SOIL*. *Soil* 1, 117–129. doi:10.5194/soil-1-117-2015
- 190 Chen, F., Fang, N., Shi, Z., 2016. Using biomarkers as fingerprint properties to identify
191 sediment sources in a small catchment. *Sci. Total Environ.* 557–558, 123–133.
192 doi:10.1016/j.scitotenv.2016.03.028
- 193 Chen, F.X., Fang, N.F., Wang, Y.X., Tong, L.S., Shi, Z.H., 2017. Biomarkers in sedimentary
194 sequences: Indicators to track sediment sources over decadal timescales. *Geomorphology*
195 278, 1–11. doi:10.1016/j.geomorph.2016.10.027
- 196 Cole, J.J., Prairie, Y.T., Caraco, N.F., McDowell, W.H., Tranvik, L.J., Striegl, R.G., Duarte,
197 C.M., Kortelainen, P., Downing, J.A., Middelburg, J.J., Melack, J., 2007. Plumbing the
198 global carbon cycle: Integrating inland waters into the terrestrial carbon budget.
199 *Ecosystems* 10, 171–184. doi:10.1007/s10021-006-9013-8
- 200 Collins, A.L., Williams, L.J., Zhang, Y.S., Marius, M., Dungait, J.A.J., Smallman, D.J., Dixon,
201 E.R., Stringfellow, A., Sear, D.A., Jones, J.I., Naden, P.S., 2013. Catchment source
202 contributions to the sediment-bound organic matter degrading salmonid spawning gravels
203 in a lowland river, southern England. *Sci. Total Environ.* 456, 181–195.
- 204 Collins, A.L., Williams, L.J., Zhang, Y.S., Marius, M., Dungait, J.A.J., Smallman, D.J., Dixon,
205 E.R., Stringfellow, A., Sear, D.A., Jones, J.I., Naden, P.S., Collins, A.L., Williams, L.J.,
206 Zhang, Y.S., Marius, M., Dungait, J.A.J., Smallman, D.J., Dixon, E.R., Stringfellow, A.,
207 Sear, D.A., Jones, J.I., Naden, P.S., 2014. Sources of sediment-bound organic matter
208 infiltrating spawning gravels during the incubation and emergence life stages of
209 salmonids. *Agric. Ecosyst. Environ.* 196, 76–93. doi:10.1016/j.agee.2014.06.018
- 210 Cooper, R.J., Pedentchouk, N., Hiscock, K.M., Disdle, P., Krueger, T., Rawlins, B.G., 2015.
211 Apportioning sources of organic matter in streambed sediments: An integrated molecular
212 and compound-specific stable isotope approach. *Sci. Total Environ.* 520, 187–197.
213 doi:10.1016/j.scitotenv.2015.03.058
- 214 Dinsdale, J., 2009. Loe Pool Catchment Management Project 2009 Review.
- 215 Eckmeier, E., Wiesenberg, G.L.B., 2009. Short-chain n-alkanes (C16-20) in ancient soil are
216 useful molecular markers for prehistoric biomass burning. *J. Archaeol. Sci.* 36, 1590–
217 1596. doi:10.1016/j.jas.2009.03.021
- 218 Eglinton, G., Gonzalez, A.G., Hamilton, R.J., Raphael, R.A., 1962. Hydrocarbon constituents
219 of the wax coatings of plant leaves: A taxonomic survey. *Phytochemistry* 1, 89–102.

- 220 Fang, J., Wu, F., Xiong, Y., Li, F., Du, X., An, D., Wang, L., 2014. Source characterization of
 221 sedimentary organic matter using molecular and stable carbon isotopic composition of n-
 222 alkanes and fatty acids in sediment core from Lake Dianchi, China. *Sci. Total Environ.*
 223 473–474, 410–21. doi:10.1016/j.scitotenv.2013.10.066
- 224 Feng, X., Gustafsson, Holmes, R.M., Vonk, J.E., Van Dongen, B.E., Semiletov, I.P., Dudarev,
 225 O. V., Yunker, M.B., MacDonald, R.W., Montluçon, D.B., Eglinton, T.I., 2015. Multi-
 226 molecular tracers of terrestrial carbon transfer across the pan-Arctic: Comparison of
 227 hydrolyzable components with plant wax lipids and lignin phenols. *Biogeosciences* 12,
 228 4841–4860. doi:10.5194/bg-12-4841-2015
- 229 Ficken, K.J., Li, B., Swain, D.L., Eglinton, G., 2000. An n-alkane proxy for the sedimentary
 230 input of submerged/floating freshwater aquatic macrophytes. *Org. Geochem.* 31, 745–
 231 749. doi:10.1016/S0146-6380(00)00081-4
- 232 Galy, V., Eglinton, T., France-Lanord, C., Sylva, S., 2011. The provenance of vegetation and
 233 environmental signatures encoded in vascular plant biomarkers carried by the Ganges-
 234 Brahmaputra rivers. *Earth Planet. Sci. Lett.* 304, 1–12. doi:10.1016/j.epsl.2011.02.003
- 235 Galy, V., Peucker-Ehrenbrink, B., Eglinton, T., 2015. Global carbon export from the terrestrial
 236 biosphere controlled by erosion. *Nature* 521, 204–207. doi:10.1038/nature14400
- 237 Glendell, M., Brazier, R.E., 2014. Accelerated export of sediment and carbon from a landscape
 238 under intensive agriculture. *Sci. Total Environ.* 476–477, 643–656.
 239 doi:10.1016/j.scitotenv.2014.01.057
- 240 Glendell, M., Extence, C., Chadd, R., Brazier, R.E., 2014a. Testing the pressure-specific
 241 invertebrate index (PSI) as a tool for determining ecologically relevant targets for
 242 reducing sedimentation in streams. *Freshw. Biol.* 59, 353–367. doi:10.1111/fwb.12269
- 243 Glendell, M., Granger, S.J., Bol, R., Brazier, R.E., 2014b. Quantifying the spatial variability
 244 of soil physical and chemical properties in relation to mitigation of diffuse water pollution.
 245 *Geoderma* 214–215, 25–41.
- 246 Graeber, D., Goyenola, G., Meerhoff, M., Zwirnmann, E., Ovesen, N.B.B., Glendell, M.,
 247 Gelbrecht, J., Teixeira de Mello, F., González-Bergonzoni, I., Jeppesen, E., Kronvang, B.,
 248 2015. Interacting effects of climate and agriculture on fluvial DOM in temperate and
 249 subtropical catchments. *Hydrol. Earth Syst. Sci.* 19, 2377–2394. doi:10.5194/hess-19-
 250 2377-2015
- 251 Guzman, G., Quinton, J.N., Nearing, M.A., Mabit, L., Gómez, J.A., 2013. Sediment tracers in
 252 water erosion studies: Current approaches and challenges. *J. Soils Sediments* 13, 816–
 253 833. doi:10.1007/s11368-013-0659-5
- 254 Hamilton, S.K., Lewis, W.M., 1992. Stable carbon and nitrogen isotopes in algae and detritus
 255 from the Orinoco River floodplain, Venezuela. *Geochim. Cosmochim. Acta* 56, 4237–
 256 4246.
- 257 Hodell, D. a, Schelske, C.L., 1998. Production, sedimentation, and isotopic composition of
 258 organic matter in Lake Ontario. *Limnol. Oceanogr.* 43, 200–214.
 259 doi:10.4319/lo.1998.43.2.0200
- 260 Laceby, J.P., Olley, J., Pietsch, T.J., Sheldon, F., Bunn, S.E., 2015. Identifying subsoil

- 261 sediment sources with carbon and nitrogen stable isotope ratios. *Hydrol. Process.* 29,
262 1956–1971. doi:10.1002/hyp.10311
- 263 Lauerwald, R., Laruelle, G.G., Hartmann, J., Ciais, P., Regnier, P.A.G., 2015. Global
264 Biogeochemical Cycles 534–554. doi:10.1002/2014GB004941.Received
- 265 Li, M., Peng, C., Wang, M., Xue, W., Zhang, K., Wang, K., Shi, G., Zhu, Q., 2017. The carbon
266 flux of global rivers: A re-evaluation of amount and spatial patterns. *Ecol. Indic.* 80, 40–
267 51. doi:10.1016/j.ecolind.2017.04.049
- 268 Ludwig, W., P. Amiotte-Suchet, J.L. Probst, F.G. Hall, G.J. Collatz, B.W. Meeson, S.O. Los,
269 E.Brown De Colstoun, and D.R.L., 2011. ISLSCP II Global River Fluxes of Carbon and
270 Sediments to the Oceans.
- 271 Loe Pool Forum 2017. <https://loepool.org/> (last accessed on 04/10/2017)
- 272 Maavara, T., Lauerwald, R., Regnier, P., Van Cappellen, P., 2017. Global perturbation of
273 organic carbon cycling by river damming. *Nat. Commun.* 8, 15347.
274 doi:10.1038/ncomms15347
- 275 Mackereth, F.J.H., 1969. Short core sampler for subaqueous deposits. *Limnol. Oceanogr.* 14,
276 145–151.
- 277 Marín-Spiotta, E., Gruley, K.E., Crawford, J., Atkinson, E.E., Miesel, J.R., Greene, S.,
278 Cardona-Correa, C., Spencer, R.G.M., 2014. Paradigm shifts in soil organic matter
279 research affect interpretations of aquatic carbon cycling: Transcending disciplinary and
280 ecosystem boundaries. *Biogeochemistry* 117, 279–297. doi:10.1007/s10533-013-9949-7
- 281 Meersmans, J., Arrouays, D., Rompaey, A.J.J. Van, Pagé, C., Baets, S. De, Quine, T.A., 2016.
282 Future C loss in mid-latitude mineral soils: climate change exceeds land use mitigation
283 potential in France. *Sci. Rep.* 6, 1–11. doi:10.1038/srep35798
- 284 Meyers, P.A., Lallier-Vergès, E., 1999. Lacustrine sedimentary organic matter of Late
285 Quaternary paleoclimates. *J. Paleolimnol.* 21, 345–372. doi:10.1023/A:1008073732192
- 286 Meyers, P. a, 2003. Application of organic geochemistry to paleolimnological reconstruction:
287 a summary of examples from the Laurention Great Lakes. *Org. Geochem.* 34, 261–289.
- 288 Mouchet, M.A., Paracchini, M.L., Schulp, C.J.E., Sturck, J., Verkerk, P.J., Verburg, P.H.,
289 Lavorel, S., 2016. Bundles of ecosystem (dis) services and multifunctionality across
290 European landscapes. *Ecol. Indic.* 73, 23–28. doi:10.1016/j.ecolind.2016.09.026. 73
- 291 Nakayama, T., 2017. Development of an advanced eco-hydrologic and biogeochemical
292 coupling model aimed at clarifying the missing role of inland water in the global
293 biogeochemical cycle. *J. Geophys. Res. Biogeosciences.*
- 294 National Trust, 2017. <https://www.nationaltrust.org.uk/features/looking-after-loe-pool> (last
295 accessed on 04/10/2007)
- 296 Norris, C.E., Dungait, J.A.J., Joynes, A., Quideau, S.A., 2013. Biomarkers of novel ecosystem
297 development in boreal forest soils. *Org. Geochem.* 64, 9–18.
- 298 Owens, P.N., Blake, W.H., Gaspar, L., Gateuille, D., Koiter, A.J., Lobb, D.A., Petticrew, E.L.,
299 Reiffarth, D.G., Smith, H.G., Woodward, J.C., 2016. *Earth-Science Reviews*

- 300 Fingerprinting and tracing the sources of soils and sediments : Earth and ocean science ,
 301 geoarchaeological , forensic , and human health applications. *Earth Sci. Rev.* 162, 1–23.
 302 doi:10.1016/j.earscirev.2016.08.012
- 303 Palazón, L., Latorre, B., Gaspar, L., Blake, W.H., Smith, H.G., Navas, A., 2015. Comparing
 304 catchment sediment fingerprinting procedures using an auto-evaluation approach with
 305 virtual sample mixtures. *Sci. Total Environ.* 532, 456–466.
 306 doi:10.1016/j.scitotenv.2015.05.003
- 307 Panagos, P., Borrelli, P., Poesen, J., Ballabio, C., Lugato, E., Meusburger, K., Montanarella,
 308 L., Alewell, C., 2015. The new assessment of soil loss by water erosion in Europe.
 309 *Environ. Sci. Policy* 54, 438–447. doi:10.1016/j.envsci.2015.08.012
- 310 Parnell, A., Jackson, A., 2008. Stable Isotope Analysis in R [WWW Document]. URL
 311 <https://cran.r-project.org/package=siar>
- 312 Puttock, A., Dungait, J.A.J., Macleod, C.J.A., Bol, R., Brazier, R.E., 2014. Woody plant
 313 encroachment into grasslands leads to accelerated erosion of previously stable organic
 314 carbon from dryland soils. *J. Geophys. Res. Biogeosciences* 119, 2345–2357.
 315 doi:10.1002/2014JG002635.Received
- 316 Ranjan, R.K., Routh, J., Val Klump, J., Ramanathan, A.L., 2015. Sediment biomarker profiles
 317 trace organic matter input in the Pichavaram mangrove complex, southeastern India. *Mar.*
 318 *Chem.* 171, 44–57. doi:10.1016/j.marchem.2015.02.001
- 319 Raymond, P. a, Hartmann, J., Lauerwald, R., Sobek, S., McDonald, C., Hoover, M., Butman,
 320 D., Striegl, R., Mayorga, E., Humborg, C., Kortelainen, P., Dürr, H., Meybeck, M., Ciais,
 321 P., Guth, P., 2013. Global carbon dioxide emissions from inland waters. *Nature* 503, 355–
 322 9. doi:10.1038/nature12760
- 323 Regnier, P., Friedlingstein, P., Ciais, P., Mackenzie, F.T., Gruber, N., Janssens, I. a., Laruelle,
 324 G.G., Lauerwald, R., Luysaert, S., Andersson, A.J., Arndt, S., Arnosti, C., Borges, A. V.,
 325 Dale, A.W., Gallego-Sala, A., Godd eris, Y., Goossens, N., Hartmann, J., Heinze, C.,
 326 Ilyina, T., Joos, F., LaRowe, D.E., Leifeld, J., Meysman, F.J.R., Munhoven, G., Raymond,
 327 P. a., Spahni, R., Suntharalingam, P., Thullner, M., 2013. Anthropogenic perturbation of
 328 the carbon fluxes from land to ocean. *Nat. Geosci.* 6, 597–607. doi:10.1038/ngeo1830
- 329 Reiffarth, D.G., Petticrew, E.L., Owens, P.N., Lobb, D.A., 2016. Sources of variability in fatty
 330 acid (FA) biomarkers in the application of compound-specific stable isotopes (CSSIs) to
 331 soil and sediment fingerprinting and tracing: A review. *Sci. Total Environ.* 565, 8–27.
 332 doi:10.1016/j.scitotenv.2016.04.137
- 333 Rickson, R.J., 2014. Can control of soil erosion mitigate water pollution by sediments? *Sci.*
 334 *Total Environ.* 468–469, 1187–1197. doi:10.1016/j.scitotenv.2013.05.057
- 335 Schmidt, M.W.I., Torn, M.S., Abiven, S., Dittmar, T., Guggenberger, G., Janssens, I. a.,
 336 Kleber, M., K ogel-Knabner, I., Lehmann, J., Manning, D. a. C., Nannipieri, P., Rasse,
 337 D.P., Weiner, S., Trumbore, S.E., 2011. Persistence of soil organic matter as an ecosystem
 338 property. *Nature* 478, 49–56. doi:10.1038/nature10386
- 339 Schoumans, O.F., Chardon, W.J., Bechmann, M.E., Gascuel-Oudou, C., Hofman, G.,
 340 Kronvang, B., Rub ek, G.H., Ul en, B., Dorioz, J.M., 2014. Mitigation options to reduce
 341 phosphorus losses from the agricultural sector and improve surface water quality: A

- 342 review. *Sci. Total Environ.* 468–469, 1255–1266. doi:10.1016/j.scitotenv.2013.08.061
- 343 Schroter, D., Cramer, W., Leemans, R., Arnell, N.W., Prentice, I.C., Arau, M.B., Bondeau, A.,
344 Bugmann, H., Carter, T.R., Gracia, C.A., Vega-leinert, A.C. De, Erhard, M., Ewert, F.,
345 Glendining, M., House, J.I., Klein, R.J.T., Lavorel, S., Kankaanpa, S., Lindner, M.,
346 Metzger, M.J., Meyer, J., Mitchell, T.D., Reginster, I., Rounsevell, M., 2005. Ecosystem
347 Service Supply and Vulnerability to Global Change in Europe.
- 348 Senbayram, M., Dixon, L., Goulding, K.W.T., B.R., 2008. Long-term influence of manure and
349 mineral nitrogen applications on plant and soil ¹⁵N and ¹³C values from the Broadbalk
350 Wheat Experiment. *Rapid Commun. Mass Spectrom.* 22, 1735–1740.
351 doi:10.1002/rcm.3548
- 352 Sherriff, S.C., Franks, S.W., Rowan, J.S., Fenton, O., Daire, Ó., 2015. Uncertainty-based
353 assessment of tracer selection , tracer non-conservativeness and multiple solutions in
354 sediment fingerprinting using synthetic and field data 2101–2116. doi:10.1007/s11368-
355 015-1123-5
- 356 Silliman, J.E., Schelske, C.L., 2003. Saturated hydrocarbons in the sediments of Lake Apopka,
357 Florida. *Org. Geochem.* 34, 253–260. doi:10.1016/S0146-6380(02)00169-9
- 358 Smith, H.G., Evrard, O., Blake, W.H., Owens, P.N., Smith, H.G., 2015. Preface — Addressing
359 challenges to advance sediment fingerprinting research 2033–2037. doi:10.1007/s11368-
360 015-1231-2
- 361 Tao, S., Eglinton, T.I., Montluçon, D.B., McIntyre, C., Zhao, M., 2016. Diverse origins and
362 pre-depositional histories of organic matter in contemporary Chinese marginal sea
363 sediments. *Geochim. Cosmochim. Acta* 191, 70–88. doi:10.1016/j.gca.2016.07.019
- 364 Team, R.C., 2014. R: A language and environment for statistical computing. R Foundation for
365 Statistical Computing, Vienna, Austria.
- 366 Tian, H., 2015. *Journal of Geophysical Research: Biogeosciences*. *J. Geophys. Res.*
367 *Biogeosciences* 120, 752–772. doi:10.1002/2014JG002760.Received
- 368 Tilman, D., Cassman, K.G., Matson, P.A., Naylor, R., Polasky, S., 2002. Agricultural
369 sustainability and intensive production practices. *Nature* 418, 671–677.
370 doi:10.1038/nature01014
- 371 Tolosa, I., Fiorini, S., Gasser, B., Martín, J., Miquel, J.C., 2013. Carbon sources in suspended
372 particles and surface sediments from the Beaufort Sea revealed by molecular lipid
373 biomarkers and compound-specific isotope analysis. *Biogeosciences* 10, 2061–2087.
374 doi:10.5194/bg-10-2061-2013
- 375 Torres, T., Ortiz, J.E., Martin-Sanchez, D., Arribas, I., Moreno, L., Ballesteros, B., Blazquez,
376 A., Dominguez, J.A., Estrealla, T.R., 2014. The long Pleistocene record from the Pero-
377 Oliva marshland (Alicante-Valencia, Spain), in: Martini, I.P., Wanless, H.R. (Ed.),
378 *Sedimentary Coastal Zones from High to Low Latitudes: Similarities and Differences*.
379 Geological Society of London, pp. 429–448.
- 380 Tranvik, L.J., Downing, J.A., Cotner, J.B., Loiselle, S.A., Striegl, R.G., Ballatore, T.J., Dillon,
381 P., Finlay, K., Fortino, K., Knoll, L.B., Kortelainen, P.L., Kutser, T., Larsen, S., Laurion,
382 I., Leech, D.M., McCallister, S.L., McKnight, D.M., Melack, J.M., Overholt, E., Porter,

- 383 J.A., Prairie, Y., Renwick, W.H., Roland, F., Sherman, B.S., Schindler, D.W., Sobek, S.,
384 Tremblay, A., Vanni, M.J., Verschoor, A.M., von Wachenfeldt, E., Weyhenmeyer, G.A.,
385 2009. Lakes and reservoirs as regulators of carbon cycling and climate. *Limnol. Oceanogr.*
386 54, 2298–2314. doi:10.4319/lo.2009.54.6_part_2.2298
- 387 Turnage, K.M., Lee, S.Y., Foss, J.E., Kim, K.H., Larsen, I.J., 1997. Comparison of soil erosion
388 and deposition rates using radiocesium, RUSLE, and buried soils in dolines in East
389 Tennessee. *Environ. Geol.* 29, 1–10.
- 390 Verheijen, F.G.A., Jones, R.J.A., Rickson, R.J., Smith, C.J., 2009. Tolerable versus actual soil
391 erosion rates in Europe. *Earth-Science Rev.* 94, 23–38.
392 doi:10.1016/j.earscirev.2009.02.003
- 393 Walling, D.E., 2013. The evolution of sediment source fingerprinting investigations in fluvial
394 systems. *J. Soils Sediments* 13, 1658–1675. doi:10.1007/s11368-013-0767-2
- 395 Wang, N., Zong, Y., Brodie, C.R., Zheng, Z., 2014. An examination of the fidelity of n-alkanes
396 as a palaeoclimate proxy from sediments of Palaeolake Tianyang, South China. *Quat. Int.*
397 333, 100–109. doi:10.1016/j.quaint.2014.01.044
- 398 Wohl, E., Hall, R.O., Lininger, K.B., Sutfin, N.A., Walters, D.M., 2017. Carbon dynamics of
399 river corridors and the effects of human alterations. *Ecol. Monogr.* 87, 379–409.
400 doi:10.1002/ecm.1261
- 401 Xu, H., Ai, L., Tan, L., An, Z., 2006. Stable isotopes in bulk carbonates and organic matter in
402 recent sediments of Lake Qinghai and their climatic implications. *Chem. Geol.* 235, 262–
403 275. doi:10.1016/j.chemgeo.2006.07.005
- 404 Yoshii, K., Wada, E., Takamatsu, N., Karabanov, E.B., Kawai, T., 1997. ^{13}C and ^{15}N
405 abundances in the sediment core (VER 921/1-St-10-GC2) from northern Lake Baikal.
406 *Isotopes Environ. Health Stud.* 33, 277–286. doi:10.1080/10256019708234038
- 407 Zech, M., Krause, T., Meszner, S., Faust, D., 2013. Incorrect when uncorrected: Reconstructing
408 vegetation history using n-alkane biomarkers in loess-paleosol sequences - A case study
409 from the Saxonian loess region, Germany. *Quat. Int.* 296, 108–116.
410 doi:10.1016/j.quaint.2012.01.023
- 411 Zech, M., Rass, S., Buggle, B., Löffler, M., Zöllner, L., 2012. Reconstruction of the late
412 Quaternary paleoenvironments of the Nussloch loess paleosol sequence, Germany, using
413 n-alkane biomarkers. *Quat. Res. (United States)* 78, 226–235.
414 doi:10.1016/j.yqres.2012.05.006
- 415 Zech, M., Zech, R., Morrás, H., Moretti, L., Glaser, B., Zech, W., 2009. Late Quaternary
416 environmental changes in Misiones, subtropical NE Argentina, deduced from multi-proxy
417 geochemical analyses in a palaeosol-sediment sequence. *Quat. Int.* 196, 121–136.
418 doi:10.1016/j.quaint.2008.06.006
- 419 Zhang, X.C. (John), Liu, B.L., 2016. Using multiple composite fingerprints to quantify fine
420 sediment source contributions: A new direction. *Geoderma* 268, 108–118.
421 doi:10.1016/j.geoderma.2016.01.031

422

Appendix 1 Biogeochemical values (mean and SD) of the 50 source soils, river bed sediments and lake core samples included in the PCA analysis. N = number of replicates.

| Land use (N) | C ₂₇ :C ₃₁ | PAQ | % C ₂₇ | % C ₂₉ | % C ₃₁ | % N | δ ¹⁵ N (‰) | % C | C/N | δ ¹³ C (‰) |
|--------------|----------------------------------|----------------|-------------------|-------------------|-------------------|----------------|-----------------------|----------------|-----------------|-----------------------|
| | Mean (SD) | | | | | | | | | |
| Arable (11) | 0.25 (0.08) | 0.09 (0.02) | 0.13 (0.04) | 0.35 (0.06) | 0.52 (0.06) | 0.33 (0.05) | 5.3 (1.03) | 3.05 (0.64) | 9.32 (0.97) | -27.6 (0.42) |
| Grass (7) | 0.37 (0.34) | 0.10 (0.04) | 0.16 (0.07) | 0.33 (0.04) | 0.51 (0.11) | 0.52 (0.10) | 5.2 (1.21) | 5.40 (1.08) | 10.39 (0.86) | -28.0 (0.57) |
| Ley (9) | 0.26 (0.10) | 0.12 (0.09) | 0.13 (0.04) | 0.34 (0.01) | 0.53 (0.04) | 0.40 (0.08) | 5.2 (0.63) | 3.77 (1.07) | 9.21 (0.86) | -28.2 (0.33) |
| Woodland (4) | 1.74 (0.54) | 0.15 (0.02) | 0.37 (0.07) | 0.41 (0.05) | 0.22 (0.04) | 0.62 (0.16) | 4.7 (1.97) | 7.80 (2.29) | 12.67 (3.23) | -28.3 (0.31) |
| River (7) | 2.21 (0.37) | 0.17 (0.03) | 0.40 (0.03) | 0.41 (0.02) | 0.19 (0.02) | 0.19 (0.06) | 4.5 (1.06) | 2.34 (0.84) | 12.20 (1.01) | -28.3 (0.24) |
| Lake (12) | 1.37 (0.37) | 0.17 (0.03) | 0.36 (0.05) | 0.37 (0.01) | 0.27 (0.05) | 0.70 (0.07) | 6.4 (0.31) | 7.61 (0.95) | 10.91 (0.46) | -27.7 (0.41) |

Tracing of particulate organic C sources across the terrestrial-aquatic continuum, a case study at the catchment scale (Carminowe Creek, southwest England)

Glendell, M.

2017-11-06

Attribution-NonCommercial-NoDerivatives 4.0 International

Liu Y, Mo D, Nalianda D, et.al., (2018) Tracing of particulate organic C sources across the terrestrial-aquatic continuum, a case study at the catchment scale (Carminowe Creek, southwest England). *Science of The Total Environment*, Volumes 616–617, March 2018, pp. 1077-1088

<https://doi.org/10.1016/j.scitotenv.2017.10.211>

Downloaded from CERES Research Repository, Cranfield University